The Natural Latitudinal Distribution of Atmospheric CO_2*

by

John A. Taylor[1] *and James C. Orr*[2]

[1]Mathematics and Computer Science Division and Environmental Research Division, Argonne National Laboratory, 9700 S. Cass Ave., Argonne, IL 60439

[2]Laboratoire des Sciences du Climat et de l'Environnement, CEA Saclay, Bat. 709 L'Orme, F-91191 Gif-sur-Yvette, France

Climate and Global Change

Series No. ANL/CGC-002-0400

April 2000

*Support for this work came in part from the EC Environment and Climate Program (contracts ENV4-CT95-0132 and ENV4-CT97-0495); from the Mathematical, Information, and Computational Sciences Division subprogram of the Office of Advanced Scientific Computing Research, U.S. Department of Energy, under Contract W-31-109-Eng-38; and a Commonwealth Fellowship via the Bede Morris Fellowship Scheme (Australian and French Academies of Science) who helped support visits of JAT to LSCE.

Contents

Abstract 1

1. Introduction 2

2. Method 5

3. Results 6

4. Discussion 8

5. Conclusions 12

References 13

Figure Captions 18

ABSTRACT

Although poorly understood, the north-south distribution of the natural component of atmospheric CO_2 offers information essential to improving our understanding of the exchange of CO_2 between the atmosphere, oceans, and biosphere. The natural or unperturbed component is equivalent to that part of the atmospheric CO_2 distribution, which is controlled by non-anthropogenic CO_2 fluxes from the ocean and terrestrial biosphere. Models should be able to reproduce the true north-south gradient in CO_2 due to the natural component before they can reliably estimate present-day CO_2 sources and sinks and predict future atmospheric CO_2. We have estimated the natural latitudinal distribution of atmospheric CO_2, relative to the South Pole, using measurements of atmospheric CO_2 during 1959-1991 and corresponding estimates of anthropogenic CO_2 emissions to the atmosphere. Key features of the natural latitudinal distribution include (1) CO_2 concentrations in the Northern Hemisphere that were lower than those in the Southern Hemisphere, (2) CO_2 concentration differences that are higher in the tropics (associated with outgassing of the oceans) than those currently measured, and (3) CO_2 concentrations over the Southern Ocean that are relatively uniform. This natural latitudinal distribution and its sensitivity to increasing fossil fuel emissions indicate that near-surface concentrations of atmospheric CO_2 in the Northern Hemisphere are naturally lower than those in the southern hemisphere. Models that find the contrary will also mismatch present-day CO_2 in the northern hemisphere and incorrectly ascribe that region as a large sink of anthropogenic CO_2

1. INTRODUCTION

Our understanding of the present day fluxes of atmospheric CO_2 remains problematic (IPCC, 1996). Large inconsistencies exist in our estimates of the flux of CO_2 between the atmosphere and the ocean and between the atmosphere and the biosphere, particularly the latter. One approach to testing hypotheses concerning fluxes of atmospheric CO_2 is to make simulations with a global atmospheric tracer-transport model, including estimates of CO_2 sources and sinks (as boundary conditions), and then to compare simulated with. measured atmospheric CO_2 concentrations (Fung et al. 1983; Keeling et al. 1989a; Taylor 1989; IPCC 1996). Lack of model-data agreement has been used to imply either ocean uptake (Keeling et al. 1989a) or anthropogenic fluxes associated with the terrestrial biosphere (Tans et al. 1990). However, model results vary widely, as illustrated by the TransCom1 study (Rayner and Law 1995; Law et al. 1996). To investigate model differences, TransCom1 separated out effects due to fossil fuel CO_2 emissions and CO_2 fluxes from the terrestrial biosphere (see Fig. 1). The majority of TransCom1 models predict roughly the same latitudinal gradient in CO_2 for a given scenario of fossil fuel emissions. Conversely, the same models disagree substantially for the biosphere-only scenario, particularly around 60^o N. The TransCom1 biosphere scenario assumes no net annual flux between the terrestrial biosphere and the atmosphere.

To help resolve these model differences, what is needed most are the initial conditions, that is, the unperturbed “natural” component of atmospheric CO_2, which is produced by nonanthropogenic CO_2 fluxes from oceans and terrestrial biosphere. This may or may not be equivalent to the preindustrial state, as will be discussed later.

Based on predicted latitudinal differences in atmospheric CO_2 concentrations (Fig. 1), previous studies have derived a wide range of estimates for the uptake of atmospheric CO_2 in the Northern Hemisphere, from 0 to 3.5 Pg C yr^{-1} (Keeling et al. 1989a; Taylor 1989; Tans et al. 1990; Denning et al. 1995). Observational evidence (Tans et al. 1990) indicates that the present-day ocean would take up little of the CO_2 required by the higher estimates. Hence the present-day terrestrial biosphere has been implicated as a sink. We show why separating the anthropogenic perturbation from the natural component of atmospheric CO_2 is crucial when determining terrestrial carbon sinks.

In a seminal study, Keeling and Heimann (1986) deduced CO_2 concentrations for the preindustrial atmosphere using modern measurements, a 1-D meridional diffusive transport model, and prescribed fossil CO_2 emissions. They found preindustrial CO_2 concentrations in the Northern Hemisphere to have been ~1 ppm lower than those in the Southern Hemisphere. They proposed a resulting northward CO_2 transport in the preindustrial atmosphere, giving three possible explications: (1) a Southern Ocean source coupled with a Northern Ocean sink, (2) a similar imbalance between sources and sinks in the terrestrial biosphere, and (3) a correlation between seasonal variations in atmospheric circulation patterns and seasonal variability of CO_2 produced by the terrestrial biosphere (Pearman and Hyson 1980). The latter effect was coined the "rectification process" by Keeling et al. (1989a, p. 313).

In subsequent work, Keeling et al. (1989b) deduced a preindustrial difference of –0.82 ppm for Mauna Loa – South Pole by extrapolating changes in the north-south difference between surface measurements of atmospheric CO_2. They estimated that this preindustrial difference implies an interhemispheric northward transport in the preindustrial atmosphere of roughly 1 Pg C yr^{-1}. To produce this latitudinal distribution in atmospheric CO_2, Keeling et al. (1989b) further reasoned that the preindustrial ocean should have transported an equivalent flux southward.

Studies that exploit ocean measurements in the Atlantic Ocean suggest that preindustrial interhemispheric ocean transport is smaller, from 0.3 to 0.5 Pg C yr^{-1} southward (Broecker and Peng 1992; Keeling and Peng 1995). A comparison of results from three ocean general circulation models show that southward oceanic carbon transport in the Atlantic is balanced by northward oceanic carbon transport in the Indian and Pacific Oceans. Thus globally, interhemispheric carbon transport by the ocean models is smaller, that is, < 0.1 Pg C yr^{-1} (Sarmiento et al. 1996; Orr, 1998; Sarmiento et al., 2000). However, this ocean model comparison did not explicitly incorporate the river loop: (i) leakage to the ocean, through rivers, of atmospheric carbon absorbed via continental erosion and photosynthesis on land, (ii) subsequent oceanic transport of riverine carbon within the ocean, and (iii) the resulting loss from the ocean back to the atmosphere. Aumont (1998) and Aumont et al. (1999) have since included the river loop in one of the ocean general circulation models involved in the aforementioned ocean model comparison. With the river loop included, the global interhemispheric transport by the ocean increased to 0.35 ± 0.1 Pg C yr^{-1}, that is, to within the range suggested by ocean measurements. In summary, both ocean model- and data-based studies indicate that the preindustrial ocean does not account for most of the 1 Pg C yr^{-1} southward transport proposed by Keeling et al. (1989a).

Likewise, these air-sea fluxes of oceanic and riverine carbon are unable to explain the north-south difference in preindustrial atmospheric CO_2 deduced by Keeling et al. (1989a). To investigate this question, Aumont et al. (1999) went one step further and installed their CO_2 fluxes as boundary conditions in TM2, a 3-D atmospheric model (Heimann, 1995). They find that CO_2 fluxes from the preindustrial ocean and river loop explain at most –0.3 ppm of the -0.82 ppm estimate from Keeling et al. (1989b) for the Mauna Loa – South Pole difference in atmospheric CO_2. This suggests that the remaining –0.5 ppm is due to the rectification effect.

In Fig. 1a, the differences between the observations and the upper group of atmospheric model estimates from TransCom1 is much more than even a 1 ppm ocean effect. The large discrepancies between model predictions are caused by differences in the representation of atmospheric transport processes, particularly in response to the exchange of atmospheric CO_2 with the biosphere (Rayner and Law 1995; Law et al. 1996). The biosphere-only component (not shown) produces a nonzero north-south latitudinal gradient at the surface. As illustrated by TransCom1, atmospheric model estimates of that latitudinal gradient vary from being largely positive to slightly negative. When a model predicts that a monitoring site's surface-level CO_2 concentration (minus that at the South Pole), for the combined fossil emissions plus terrestrial biosphere simulations, is higher than that observed, either (i) important CO_2 sinks or sources have been neglected or (ii) model artifacts exist.

We suggest here that the model-artifact issue illustrated by TransCom1 has not been resolved. Until it has, predictions from atmospheric modeling studies remain inconclusive regarding the possibility of a large terrestrial sink in the Northern Hemisphere. The only sure remedy to this dilemma is to develop an improved understanding of the natural component of atmospheric CO_2. This paper takes a step in that direction, by offering a more detailed data-based analysis of trends in atmospheric CO_2.

2. METHOD

Previously, the same approach was taken to derive the preindustrial difference between Mauna Loa and the South Pole of –0.82 ppm (Keeling et al., 1989b, Siegenthaler and Sarmiento 1993). Here we have extended this work to multiple stations. Thus we are able to investigate latitudinal distribution of the natural component and its sensitivity to fossil fuel emissions. We derived the latitudinal surface distribution of the natural component in atmospheric CO_2 using (1) estimates of CO_2 fluxes from fossil fuel combustion and cement production (Marland et al. 1994) during 1959-1991 and (2) corresponding atmospheric CO_2 measurements obtained by the Scripps Institute of Oceanography (SIO) (Keeling and Whorf 1994), USA; the Climate Modeling and Diagnostics Laboratory (CMDL) (Conway et al. 1994), USA; Centre des Faibles Radioactivités (CFR) (Gaudry et al. 1994), France; National Institute of Water and Atmospheric Research Ltd. (NIWAR) (Manning et al. 1994), New Zealand; and Atmospheric Environment Service (AES) (Trivett et al. 1994), Canada. We have employed available data sets, 26 in total, from monitoring sites with at least ten-year records. Only pre-1991 data were used in order to avoid complications subsequent to the eruption of Mt. Pinatubo. That event is known to have affected both latitudinal distribution and growth rate of atmospheric CO_2 (Keeling et al. 1996). Our analysis computes mean trends and thus averages out interannual variability (Francey et al. 1995; Ciais et al. 1995).

For the years when CO_2 measurements were available, we calculated for each site the normalized difference χ_D (in ppm) relative to the South Pole. That is, χ_D is defined as the annual mean CO_2 concentration at each monitoring site minus that at the South Pole. Then for each monitoring site, we fit χ_D at as a linear function of f_{CO2}, the global flux of fossil CO_2 (in Pg C yr^{-1} , where 1 Pg C = 10^{15}g). Thus

$$\chi_D = \alpha f_{CO2} + \beta,$$

where the slope α (in ppm/Pg C yr^{-1}) reflects the sensitivity of a given site's CO_2 concentration (minus that at the South Pole) to the global flux of fossil CO_2, and the intercept β (in ppm) represents the gradient between the monitoring site and the South Pole, if there were no fossil CO_2 emissions.

3. RESULTS

Results here are entirely data based. Assumptions of this analysis are that (i) the relationship between normalized site concentration is linear with respect to the rate of global industrial emissions and that (ii) the extrapolated flux at zero fossil carbon emissions is representative of the natural gradient in atmospheric CO_2. Figure 2a illustrates the relationship for the Mauna Loa Observatory minus the South Pole difference (the monitoring sites for which the longest records of CO_2 measurements are available). The good correlation (r = 0.92) over the range 2.7 Pg C yr^{-1} to 6.2 Pg C yr^{-1} (1959-1991) indicates that the net source-sink terms for atmospheric CO_2 in the Northern Hemisphere responded linearly to fossil fuel emissions over a range that is more than half the 1991 level of emissions.

As a simple test of linearity for the period 1959-1991, we calculated the natural difference β for Mauna Loa – South Pole, using selected sets of the 27 available SIO data points. With the entire SIO data set, the calculated natural gradient β is -0.8 ± 0.2 ppm. With only fourteen data points from 1977 to 1990 (the typical range for other stations), β becomes -2.0 ± 0.6 ppm; excluding El-Niño years changes the result by less than 0.3 ppm. The 1.2 ppm difference may imply a small bias when using the shorter vs. the longer records; however, 2σ error bars do overlap, and both estimates are significantly negative to beyond the 3σ level. Randomly choosing from 9 to 20 contiguous SIO data points produces β's that range from 0.45 to -2.6 ppm. For comparison, CMDL data from the same two stations (14 years of data spanning 1977 to 1990) yields a β of -1.0 ± 1.0 ppm, in close agreement with the SIO-based estimate.

The assumption is that the response of the gradient is linear with respect to fossil fuel CO_2 emissions. Although atmospheric CO_2 measurements have been collected over a relatively short time period, a few records do span more than half of the increase in the flux of fossil CO_2 emissions to the atmosphere. Shipboard and land-based (Mauna Loa and Point Barrow) atmospheric CO_2 measurements (Bacastow and Keeling 1981) indicate that in the early 1960s between 15 and 30^{o}N, the interhemispheric gradient was close to zero (Fig. 3). For comparison we also include our predicted gradient of atmospheric CO_2 for the year 1962 (~2.7 Pg C yr^{-1}), based on the parameters derived from the linear regression (β in Fig 4a, and α in Fig 4b).

Figure 4a shows our estimates of β, the preindustrial/natural concentration relative to that at the South Pole. The smallest error bars are found for stations where atmospheric CO_2 is monitored continuously (all SIO, CFR, NIWAR, and CMDL as marked). All reported measurements are included in this analysis, except for CMDL's 1975 point at Pt. Barrow compiled from continuous measurements: we assumed this point to be an outlier based on the improvement in the Pt. Barrow - South Pole correlation coefficient (from r=.48 to r=.72) when it was removed. Observed Southern Hemisphere concentrations were not significantly different from that at the South Pole. The observed equatorial bulge in our data-based estimate of β is due to ocean outgassing of CO_2. The oceanic carbon comes from upwelling of carbon-rich deeper waters to the surface and loss of riverine carbon from the ocean. Excluding the tropical bulge, there are fifteen stations in the Northern Hemisphere. Five of these are statistically indistinguishable from zero; the other ten are all negative. Unfortunately, individual uncertainties are quite large. However, when taken together all estimates give a consistent picture: the nonperturbed Northern Hemisphere naturally has a lower CO_2 concentration than does the Southern Hemisphere.

Figure 4b presents the estimates of the slope α, the response of the CO_2 concentration difference (relative to the South Pole) to the global fossil fuel CO_2 flux, at each monitoring site. Positive values indicate that the gradient between the South Pole and the monitoring site increases with rising fossil CO_2 emissions. Negative values over the tropics indicate that the gradient between the tropics and the South Pole has decreased with increasing emissions of fossil CO_2. The sensitivity of the latitudinal concentration difference in atmospheric CO_2 to fossil fuel emissions is greatest over the major source regions in the Northern Hemisphere. With the exception of the estimates in the tropics, the α values match the range of model predicted sensitivities obtained in the TransCom1 fossil fuel experiment (Rayner and Law 1995; Law et al. 1996). This match implies that only a small additional source or sink is required in order to explain the observed change in the gradient for the period 1959–1991 and that the linear assumption is reasonable. Furthermore, we observe a strong correlation between α (Fig 4b) and β (Fig 4a), probably because of the local coincidence of the maximum release of fossil emissions and the maximum seasonal amplitude of the seasonal cycle of atmospheric CO_2 (due essentially to the exchange with the terrestrial biosphere). Both occur at similar latitudes in the Northern Hemisphere.

4. DISCUSSION

Our interpretation that the nonperturbed Northern Hemisphere naturally has a lower CO_2 concentration than the Southern Hemisphere is at odds with biosphere-only results from most atmospheric models. However, atmospheric models can produce concentrations lower in the Northern Hemisphere (Pearman and Hyson, 1980; Taylor, 1989; Hunt et al., 1996). One explanation for lower Northern Hemisphere concentrations is that the seasonal variation in wind speed can have a greater effect on the seasonal cycle of surface atmospheric CO_2 than does the seasonal variation in the planetary boundary layer (PBL) height and cloud transport, thereby producing lower concentrations in the Northern Hemisphere than in the Southern Hemisphere (Taylor, 1998). Conversely, the seasonal variation of PBL height tends to produce higher concentrations in the northern vs. southern hemisphere (Denning, 1995).

In the biosphere-only scenario of TransCom1 (Rayner and Law 1995; Law et al. 1996), the twelve global 3-D atmospheric models predict latitudinal gradients in atmospheric CO_2 that vary significantly (from -1 to +3 ppm). These discrepancies arise from the different model responses to the large seasonal variability in the fluxes of CO_2 from the biosphere. This biospheric oscillation manifests itself in the twelve models by generating up to a 50 ppm, zonally averaged, seasonal cycle at midlatitudes in the Northern Hemisphere. Discrepancies between models are caused by differences in the ways the models represent the planetary boundary layer, advection, and vertical mixing (Denning et al. 1995; Taylor, 1998). Figure 4a illustrates this 4 ppm difference by including results from three representative TransCom1 models: ANU (Taylor 1989), CSU (Denning et al. 1995) and GISS (Fung et al. 1987). All TransCom1 models used the same scenario for biospheric CO_2 fluxes (Fung et al. 1987). Results from the TransCom1 models imply that if there were substantially higher CO_2 concentrations in the Northern Hemisphere due to natural processes, then there must exist a large sink of CO_2 (>3 Pg C yr^{-1}) in the midnorthern latitudes, in order that models match the present-day CO_2 gradient in atmospheric CO_2 (Denning et al. 1995); conversely, natural surface concentrations that were slightly lower in the Northern Hemisphere implies that that region acts today as only a small sink for CO_2 (<0.5 Pg C yr^{-1}) (Taylor 1989). Our data-based estimate of the natural north-south difference in surface atmospheric CO_2 (Fig. 4a) is negative, with the upper end of error bars reaching zero difference.

Motivated by an early presentation of this work, Conway and Tans (1999) have made a similar analysis using a more selective set of sites and longer time series. They find comparable results. Yet, their principal conclusion is opposite to our own. Conway and Tans (1999) argue that their negative data-based β in the Northern Hemisphere is consistent with a large contemporary sink in that region, whereas we argue for at most a small modern sink. We rely only on data-based estimates for β; Conway and Tans go further by comparing their β with simulated results from selected TransCom1 models (annual biosphere simulations), that is, those with positive normalized concentrations in the Northern Hemisphere. Their interpretation depends on their choice of simulated results, for which large errors have not been ruled out. That is, Conway and Tans assume that their chosen model estimates as well as the data-based β's are correct; therefore, they must interpret the large difference in the midlatitudes of the Northern Hemisphere as a large contemporary sink that is not strongly related to fossil emissions. The extrapolation technique used to determine β removes anthropogenic sinks, which scale with fossil emissions. It is difficult, then, to invoke such sinks as CO_2 fertilization and N deposition, unless these effects have already become saturated.

When considering whether our natural component β is equivalent to the preindustrial gradient, one must take into account that a nonlinear relationship between χ_D and f_{CO2} may have existed prior to 1959. Possible sources of nonlinearity include the decrease in the airborne fraction of CO_2 since preindustrial times (Bacastow and Keeling 1981), a change in patterns of sources and sinks in the ocean and biosphere (Sarmiento et al. 1992; Keeling et al. 1995), the representation of CO_2 site measurements of the mean latitudinal gradient (Ramonet and Monfray 1996), and the response of changes in atmospheric circulation to changes in climate. Some of these factors may account for part of the variability about the line shown in Fig. 2a.

A larger airborne fraction prior to 1860 (Bacastow and Keeling 1981) implies a longer residence time for anthropogenic CO_2 in the atmosphere and thus greater homogeneity. These changes in the airborne fraction may have caused the preindustrial gradient to tend more toward zero, relative to our estimate for the natural gradient, but the sign would not have changed (i.e., the preindustrial gradient should still have been negative). Changes in the airborne fraction prior to 1860 were due mostly to deforestation (Bacastow and Keeling 1981); during that same time, fossil CO_2 emissions were much smaller (<0.1 Pg C yr^{-1}). In any case, accounting for modern deforestation appears unnecessary (Fig. 2b).

Three 3-D global ocean models simulate that preindustrial CO_2 fluxes from the atmosphere to the ocean were relatively small (Sarmiento et al. 2000). Preindustrial air-sea ocean fluxes in the Northern Hemisphere appear roughly in balance with global deforestation estimates (~0.5 Pg C yr^{-1}); see (Houghton 1995). Anthropogenic air-sea

CO_2 fluxes north of 30°N represent a small fraction of fossil emissions (0.3 to 0.5 Pg C yr^{-1} in 1990) according to four ocean models (Orr 1998; Orr et al. 2000); ocean fluxes elsewhere are somewhat larger (up to 1.1 Pg C yr^{-1} in the southern ocean).

In Fig. 4b only a small change in the slope α is produced in the Southern Hemisphere for two reasons: (1) the ocean sink for anthropogenic CO_2 is largest in that region (Sarmiento et al. 1992; Orr 1998; Caldeira and Duffy, 2000; Orr et al., 2000), and (2) the fossil carbon source is mostly in the Northern Hemisphere (atmospheric mixing results in more homogenous concentrations of anthropogenic CO_2 as one moves away from the source). Over the tropical oceans, increasing fossil CO_2 emissions have generated a drop in the CO_2 gradient relative to the South Pole. The rise in atmospheric CO_2 has brought the atmosphere and tropical ocean closer to equilibrium, thus producing a drop in the CO_2 flux to the atmosphere from that region. Furthermore, the tropical ocean is a large sink of anthropogenic CO_2 (Sarmiento et al. 1992; Orr et al., 2000). Additionally, there may be a net CO_2 uptake by the tropical biosphere due to CO_2 fertilization exceeding CO_2 loss from tropical deforestation (Bacastow and Keeling 1981; Taylor and Lloyd 1992; Grace et al. 1995).

From the sensitivity α (Fig. 4b), we deduce that these relatively small changes would alter our estimates of β by less than 1 ppm, an uncertainty that falls within the error bars of our β estimates (Fig. 4a). The linear assumption requires further investigation, ideally with simulations that combine state-of-the-art carbon-cycle models of the atmosphere, ocean, and biosphere. Atmospheric models that simulate a natural component having normalized concentrations that are positive in the Northern Hemisphere interpret modern CO_2 measurements to imply a large contemporary sink in that region. Conversely, we estimate the opposite trend from data. Furthermore, we know of no processes that could effect a long-term reversal in the observed trend (equal but opposite slope α) as would be required if a large positive latitudinal gradient in CO_2 were to have existed prior to industrialization.

For the slope α, the results and interpretation of Conway and Tans (1999) are consistent with our own. Specifically, the data-based α is roughly equivalent to what most TransCom1 models predict when driven only by fossil emissions. Thus both studies agree that there has been little change in uptake of anthropogenic CO_2 by the Northern Hemisphere over the past forty years. Although α indicates the sensitivity of local atmospheric CO_2 to net sources minus sinks, it cannot be used by itself to indicate the magnitude of the sink. With their results for α, Conway and Tans (1999) suggest that the Northern Hemispheric anthropogenic sink has been large but essentially constant over the past forty years. While this is possible, little change in the sink is also consistent with a small sink of atmospheric CO_2 in the Northern Hemisphere. Given that fossil fuel emissions have increased by nearly a factor of 2 over the period of our analysis, we consider the small-sink hypothesis to be more likely.

5. CONCLUSIONS

We have estimated the natural component of the north-south gradient in atmospheric CO_2 by assuming a linear relationship between atmospheric CO_2 and emissions of fossil CO_2 (Fig. 4a). The resulting CO_2 concentrations are lower in the Northern Hemisphere than those in the Southern Hemisphere. Although uncertainties associated with individual sites are large, their combined weight suggests that it is unlikely that a large positive latitudinal gradient in atmospheric CO_2 is produced as a result of the natural component β.

Our estimate for the natural component of the latitudinal distribution for atmospheric CO_2 concentrations, normalized to that at the South Pole, may differ from that during preindustrial time, if nonlinearities in atmospheric transport and fluxes of CO_2 have played a substantial role prior to the modern CO_2 record. Nonetheless, our conclusions do not depend on the natural gradient being equivalent to the preindustrial gradient. Our understanding of the natural gradient would improve with longer time series and more monitoring sites, particularly where CO_2 is measured continuously.

To properly quantify the role of processes that drive the global carbon cycle, we need to refine estimates for the natural distribution of atmospheric CO_2. Those atmospheric models that predict that the modern terrestrial biosphere sequesters large amounts of anthropogenic carbon in the Northern Hemisphere all predict that the natural component of atmospheric CO2 due to the terrestrial biosphere is responsible for a large positive gradient in atmospheric CO_2. For example, provocative estimates of Fan et al. (1998), which suggest that North America was a sink of 1.7 ± 0.5 Pg C yr^{-1} of carbon from 1988 to 1992, derive from such a model Properly taking into account the natural gradient would help resolve the large difference between Fan et al. (1998) and Houghton et al. (1999), who estimate that North America absorbed 0.08 to 0.28 Pg C yr^{-1} during the 1980s, based on historical forestry data and a terrestrial carbon cycle model.

REFERENCES

Aumont, O., 1998. Etude du cycle naturel du carbone dans un modèle 3D de l'océan mondial, Thesis, Doctorat, Paris VI.

Aumont, O., Orr, J. C., Monfray, P., Ludwig, W., Amiotte-Suchet, P., Probst, J.-L., 1999. Riverine-driven interhemispheric transport of carbon, preprint.

Bacastow, R. B., Keeling, C. D., 1981. Pioneer effect correction to the observed airborne fraction. In: Carbon Cycle Modelling. B. Bolin (ed.), John Wiley and Sons, Chichester, pp. 247-248.

Broecker, W. S, Peng T.-H., 1992. Interhemispheric transport of carbon dioxide by ocean circulation. Nature, 356, 587-589

Caldeira, K., Duffy, P. B., 2000. The role of the Southern Ocean in uptake and storage of anthropogenic carbon dioxide. Science, 287, 620-622.

Ciais, P., Tans, P. P., Trolier, M., White, J. W. C., Francey, R. J., 1995. A large northern hemisphere terrestrial CO_2 sink indicated by the $^{13}C/^{12}C$ ratio of atmospheric CO_2. Science, 269, 1098-1102.

Conway, T. J., and Tans, P. P., 1999. Development of the CO_2 latitude gradient in recent decades. Global Biogeochem. Cycles, 13, 821-826.

Conway, T .J., Tans, P. P., Waterman, L. S., 1994. Atmospheric CO_2 records from sites in the NOAA/CMDL air sampling network. In: T. A. Boden, D. P. Kaiser, R. J. Sepanski,

F. W. Stoss (eds.), Trends '93: A Compendium of Data on Global Change. CDIAC, Oak Ridge National Laboratory, Oak Ridge, pp. 41-119.

Denning, A. S., Fung, I. Y., Randall, D. A., 1995. Gradient of atmospheric CO_2 due to seasonal exchange with land biota. Nature, 376, 240-243.

Fan, S., Gloor,M., Mahlman, J., Pacala, S., Sarmiento, J., Takahashi, T., Tans, P., 1998. A large terrestrial carbon sink in North America implied by atmospheric and oceanic carbon dioxide data and models. Science, 282(5388), 442-446.

Francey, R .J., Tans, P. P., Allison, C. E., Enting, I. G., White, J. W. C., Trollier, M., 1995. Changes in oceanic and terrestrial carbon uptake since 1982. Nature, 373, 326-330.

Fung, I. Y., Prentice, K., Matthews, E., Lerner, J., Russell, G., 1983. Three-dimensional tracer model study of atmospheric CO_2: Response to seasonal exchanges with the terrestrial biosphere. J. Geophys. Res., 88, 1281-1294.

Fung, I. Y., Tucker, C. J., Prentice, K. C., 1987. Application of advanced very high resolution radiometer vegetation index to study atmosphere-biosphere exchange of CO_2. J. Geophys. Res., 92, 2999-3015.

Gaudry, A., Monfray, P., Bonsang, G., Kazan, V., Polian, G., Lambert, G., 1994. Atmospheric CO_2 record from in situ measurements at Amsterdam Island. In: T. A. Boden, D. P. Kaiser, R. J. Sepanski, F. W. Stoss (eds.), Trends '93: A Compendium of Data on Global Change. CDIAC, Oak Ridge National Laboratory, Oak Ridge, 1994, pp. 131-134.

Grace, J., Lloyd, J., McIntyre, J., Miranda, A.C., Meir, P., Miranda, H. S., Nobre, C., Moncrieff, J., Massheder, J., Malhi, Y., Wright, I., Gash, J., 1995. Carbon dioxide uptake by an undisturbed tropical rain forest in Southwest Amazonia, 1992 to 1993. Science, 270, 778-780.

Heimann, M., 1995. The TM2 tracer model, model description and user manual, Deutsches Klimarechenzentrum 10, 47.

Heimann, M., Keeling, C. D., Fung, I. Y., 1986. Simulating the atmospheric carbon dioxide distribution with a three-dimensional tracer model, in J. R. Travalka, D. E. Reichle (eds.), The Changing Carbon Cycle: A Global Analysis, Springer Verlag, New York, pp. 16-49.

Houghton, R.A., 1996. Terrestrial sources and sinks of carbon inferred from terrestrial data. Tellus, 48B, 420-432.

Houghton, R.A., Hackler, J. L., Lawrence, K. T. 1999. The U.S. carbon budget: Contributions from land-use change. Science, 285, 574-578.

Hunt, E. R., Piper, S. C., Nemani, R., Keeling, C. D., Otto, R. D., Running, S. W., 1996. Global net carbon exchange and intra-annual atmospheric CO_2 concentrations predicted by an ecosystems process model and three-dimensional atmospheric transport model. Global Biogeochem. Cycles, 10, 431-456.

IPCC WGI, 1996. Climate Change 1995: The Science of Climate Change - Summary for Policy Makers and Technical Summary of the Working Group I Report. R.A. Houghton et al.(eds).,Cambridge Univ. Press, Cambridge, pp. 18-21.

Keeling, C. D., Heimann, M., 1986., Meridional eddy diffusion model of the transport of atmospheric carbon dioxide 2. Mean annual carbon cycle. J Geophys. Res., 91, 7782-7796.

Keeling, C. D., Piper, S. C., Heimann, M., 1989a. A three dimensional model of atmospheric CO_2 transport based on observed winds: 4, Mean annual gradients and interannual variations. In: D. H. Peterson (ed.), Aspects of Climate Variability in the Pacific and Western Americas, Geophys. Monogr. 55, American Geophysical Union, Washington, D.C., pp 305-363

Keeling, C. D., Bacastow, R. B., Carter, A. F., Piper, S. C., Whorf, T. P., Heimann, M., Mook, W. G., Roeloffzen, H., 1989b. A three-dimensional model of atmospheric CO_2 transport based on observed winds: 1, Analysis of observational data. In: D. H. Peterson (ed.) Aspects of Climate Variability in the Pacific and Western Americas. Geophys. Monogr. 55, American Geophysical Union, Washington, D.C., pp. 165-236.

Keeling, C. D., Whorf, T. P., 1994. Atmospheric CO_2 records from sites in the SIO air sampling network. In: T. A. Boden, D. P. Kaiser, R. J. Sepanski, F. W. Stoss (eds.), Trends '93: A Compendium of Data on Global Change. CDIAC, Oak Ridge National Laboratory, Oak Ridge, pp. 16-26.

Keeling, C. D., Whorf, T. P., Wahlen, M., van der Plicht, J., 1995. Interannual extremes in the rate of rise of atmospheric carbon dioxide since 1980. Nature, 375, 666-670

Keeling, R. F., Peng, T.-H., 1995. Transport of heat, CO_2, and O_2 by the Atlantic's thermohaline circulation. Phil. Trans. R. Soc. Lond. B, 348, 133-142.

Keeling, R. F., Piper, S. C., Heimann, M., 1996. Global and hemispheric CO_2 sinks deduced from changes in atmospheric O_2 concentration. Nature, 381, 218-221

Law, R. M., Rayner, P. J., Denning, A. S., Erickson III, D., Fung, I. Y., Heimann, M., Piper, S. C., Ramonent, M., Taguchi, S., Taylor, J. A., Trudinger, C. M., Watterson, I. G., 1996. Variations in modeled atmospheric transport of carbon dioxide and consequences for CO_2 inversions. Global Biogeochem Cycles, 10, 783-796.

Ludwig, W., Probst, J. L., Kemp, S., 1996. Predicting the oceanic input of organic carbon by continental erosion. Global Biogeochem Cycles, 10, 23-41.

Manning, M. R., Gomez, A. J., Pohl, K. P., 1994. Atmospheric CO_2 record from in situ measurements at Baring Head. In: T. A. Boden, D. P. Kaiser, R. J. Sepanski, F. W. Stoss (eds.), Trends '93: A Compendium of Data on Global Change. CDIAC, Oak Ridge National Laboratory, Oak Ridge, pp. 174-178.

Marland, G., Andres, R. J., Boden, T. A., 1994. Global, regional and national CO_2 emissions. In: : T. A. Boden, D. P. Kaiser, R. J. Sepanski, F. W. Stoss (eds.), Trends '93: A Compendium of Data on Global Change. CDIAC, Oak Ridge National Laboratory, Oak Ridge, pp. 505-584.

Orr, J. C., 1998. Ocean carbon-cycle model intercomparison project (OCMIP): Phase I (1995-1997), IGBP/GAIM Report Series, Report #7, GAIM Office, University of New Hampshire, Durham.

Orr, J. C., Monfray, P., Maier-Reimer, E., Mikolajewicz, U., Palmer, J., Taylor, J., Toggweiler, J. R., Sarmiento, J. L., Le Quéré, C., Gruber, N., Sabine, C. L., Key, R. M., Boutin, J., 2000. Estimates of anthropogenic carbon uptake from four 3-D ocean models, preprint.

Pearman, G. I., Hyson, P. J., 1980. Activities of the global biosphere as reflected in atmospheric CO_2 records. J. Geophys. Res., 85, 4468-4474.

Ramonet, M., Monfray, P., 1996. CO_2 baseline concept in 3-D atmospheric transport models. Tellus 48B, 502-520.

Rayner, P. J., Law, R. M., 1995. A comparison of modelled responses to prescribed CO_2 sources. Tech. Paper No.88, CSIRO Div. of Atmos. Res., Melbourne.

Sarmiento, J. L., Maier-Reimer, E., Monfray, P., Orr, J. C., Takahashi, T., 1996. Inter-hemispheric transport of carbon in the ocean. EOS, 77, F407.

Sarmiento, J. L., Monfray, P., Maier-Reimer, E., Aumont, O., Murnane, R., Orr, J. C., 2000. Air-sea CO_2 fluxes and carbon transport: a comparison of three ocean general circulation models. Glob. Biogeochem. Cycles, in press.

Sarmiento, J. L., Murnane, R., Le Quéré, C., 1995. Air-sea transfer and the carbon budget of the North Atlantic. Phil. Trans. R. Soc. Lond., B 348, 211-219.

Sarmiento, J. L., Orr, J. C., Siegenthaler, U., 1992. A perturbation simulation of CO_2 uptake in an ocean general circulation model. J Geophys. Res., 97, 3621-3645.

Sarmiento, J. L., Sundquist, E., 1992. Revised budget for the oceanic uptake of anthropogenic carbon dioxide. Nature, 356, 589-593.

Siegenthaler, U., Sarmiento, J. L., 1993. Atmospheric carbon dioxide and the ocean. Nature, 365, 119-125.

Tans, P. P., Fung, I. Y., Takahashi, T., 1990. Observational constraints on the global atmospheric CO_2 budget. Science, 247, 1431-1438.

Taylor, J. A., 1989. A stochastic Lagrangian atmospheric transport model to determine global CO_2 sources and sinks: A preliminary discussion. Tellus, 41B, 272-285.

Taylor, J. A., Lloyd, J. L., 1992. Sources and sinks of atmospheric CO_2. Aust. J. Botany, 40, 407-418.

Taylor, J. A., 1998. Atmospheric mixing and the CO_2 seasonal cycle, Geophys. Res. Lett., 25, 4173-4176.

Trivett, N. B. A., Hudec, V. C., Wong, C. S., 1994. Atmospheric CO_2 records from sites in the AES air sampling network. In: T. A. Boden, D. P. Kaiser, R. J. Sepanski, F. W. Stoss (eds.), Trends '93: A Compendium of Data on Global Change. CDIAC, Oak Ridge National Laboratory, Oak Ridge, pp .120-130.

FIGURE CAPTIONS

Figure 1a. The latitudinal gradient in atmospheric CO_2 as measured in 1985 by CMDL (Conway et al. 1994)) (filled triangles) and as estimated from 11 atmospheric tracer transport models (TransCom1) as the sum of the average latitudinal gradients from two simulations: (i) the fossil-only run with a 5.3 Pg C yr^{-1} source, i.e., the average fossil fuel emissions of atmospheric CO_2 for the period 1980-1989, and (ii) the biosphere-only run, where every grid point has no annually averaged net source or sink of CO_2.

Figure 1b. Same as Fig. 1a except observations are from 1962 and model results are scaled to the 1962 fossil emissions of 2.7 Pg C yr^{-1}. Differences between the observed gradient and a model's prediction are used as the basis for inferring additional sources and sinks of atmospheric CO_2 associated with the oceans and the biosphere.

Figure 2a. The difference in annual averaged atmospheric CO_2 concentration between Mauna Loa Observatory, Hawaii, minus the South Pole (from measurements reported by Keeling and Whorf (1994)) plotted against the corresponding total annual flux of CO_2 emissions due to fossil fuel combustion and cement production (Marland et al. 1994). The slope α (0.50±0.04 ppm/Pg C) and the intercept β (-0.76±0.20 ppm) were estimated by linear regression (r = 0.924). Our β agrees with previous estimates using the same technique (Keeling et al., 1989b, Siegenthaler and Sarmiento 1993).

Figure 2b. As in Fig. 2a, except that the abscissa includes emissions of CO_2 due to deforestation and land use change, in addition to those from fossil fuel combustion plus cement production. Results for α (0.44±0.04 ppm/Pg C), β (-1.11±0.24 ppm) and r (0.918) are similar. Lack of improvement in the correlation suggests that modern deforestation is not a significant factor when determining the change in the gradient of atmospheric CO_2 between the South Pole and Mauna Loa Observatory.

Figure 3. The predicted latitudinal gradient in atmospheric CO_2 for the year 1962 (as in Fig. 2), compared with shipboard and land-based atmospheric CO_2 measurements as reported by Keeling et al. (1989b). Each extrapolated point is derived from the regression of the fossil CO_2 emissions vs. the difference in atmospheric CO_2 between selected monitoring sites (operated by CMDL, SIO, NIWAR, AES, and CFR) and the South Pole using the parameters as shown in Figs. 4a and 4b and where the fossil CO_2 emissions in 1962 are ~2.7 Pg C yr^{-1}. Error bars represent $\pm 1\sigma$ uncertainties. Consistent differences appear between 30°N and 70°N, but there is no data from 1962 in that region to constrain the relationship, which is shown as being linear.

Figure 4a. The natural latitudinal gradient in atmospheric CO_2 (β). Each point is derived from the regression of the fossil CO_2 emissions vs. the difference in atmospheric CO_2 between selected monitoring sites (operated by CMDL, SIO, NIWAR, AES, and CFR) and the South Pole. The three curves represent the results from the TransCom1 biosphere experiment for the CSU, GISS, and ANU models (Rayner and Law 1995; Law et al. 1996).

Figure 4b. The sensitivity of the latitudinal gradient in atmospheric CO_2 to fossil fuel emissions (α). In both plots, error bars represent $\pm 1\sigma$ uncertainties.

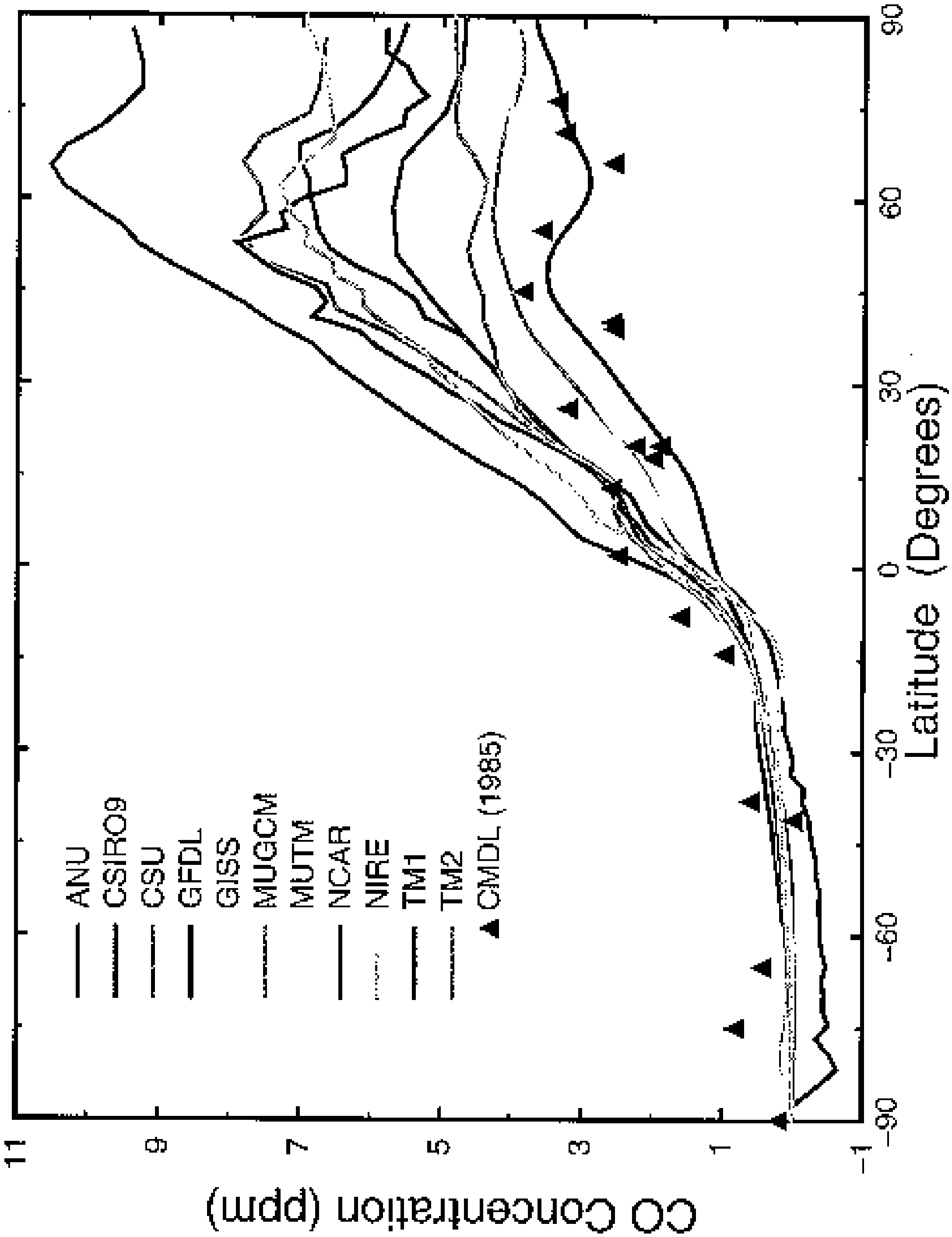

ANU
CSIRO9
CSU
GFDL
GISS
MUGCM
MUTM
NCAR
NIRE
TM1
TM2
CMDL (1985)
CO Concentration (ppm)
Latitude (Degrees)
−90
−60
−30
0
30
60
90
−1
1
3
5
7
9
11

Figure 1a

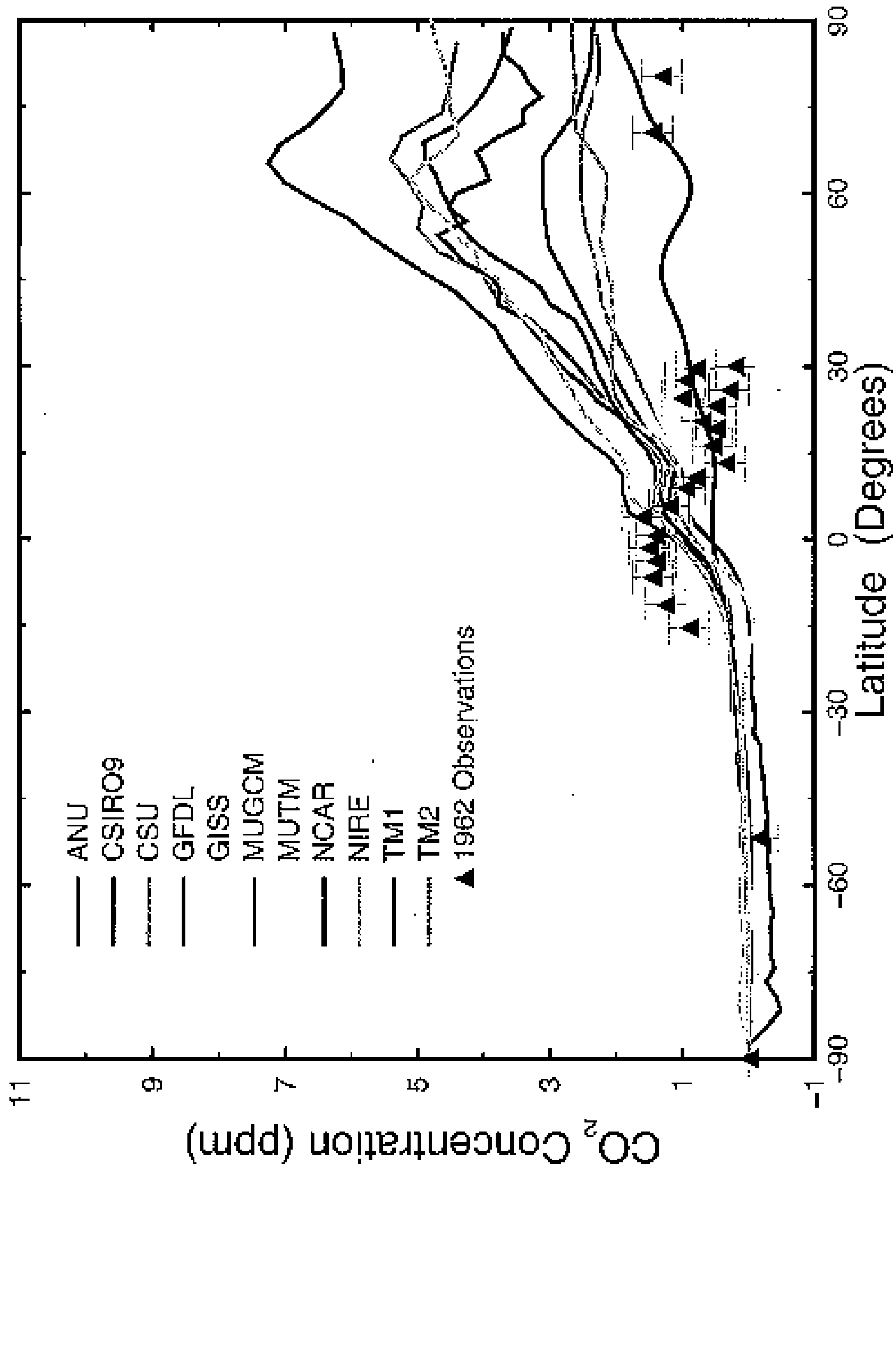

ANU
CSIRO9
CSU
GFDL
GISS
MUGCM
MUTM
NCAR
NIRE
TM1
TM2
1962 Observations
CO_2 Concentration (ppm)
Latitude (Degrees)
−1
1
3
5
7
9
11
−90
−60
−30
0
30
60
90

Figure 1b

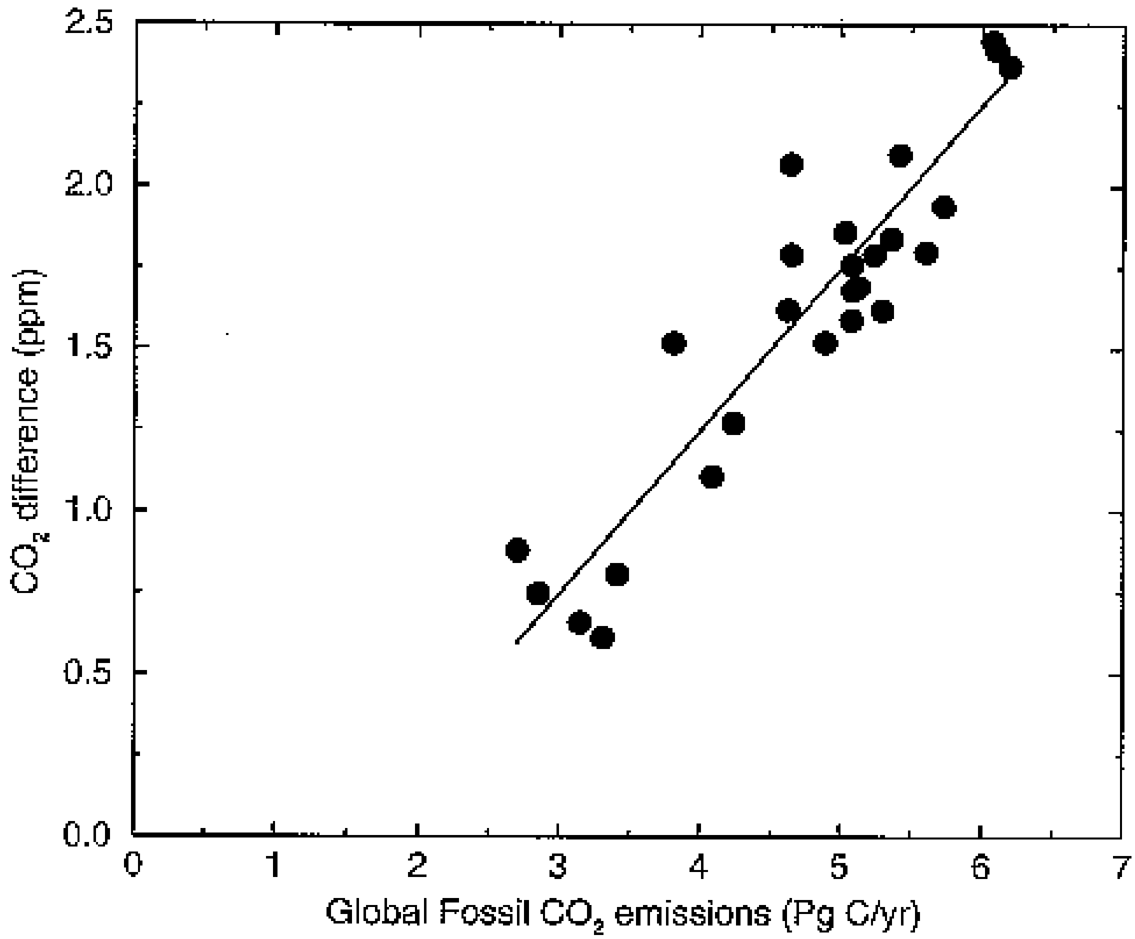
2.5
2.0
1.5
1.0
0.5
0.0
CO_2 difference (ppm)
0
1
2
3
4
5
6
7
Global Fossil CO_2 emissions (Pg C/yr)

Figure 2a

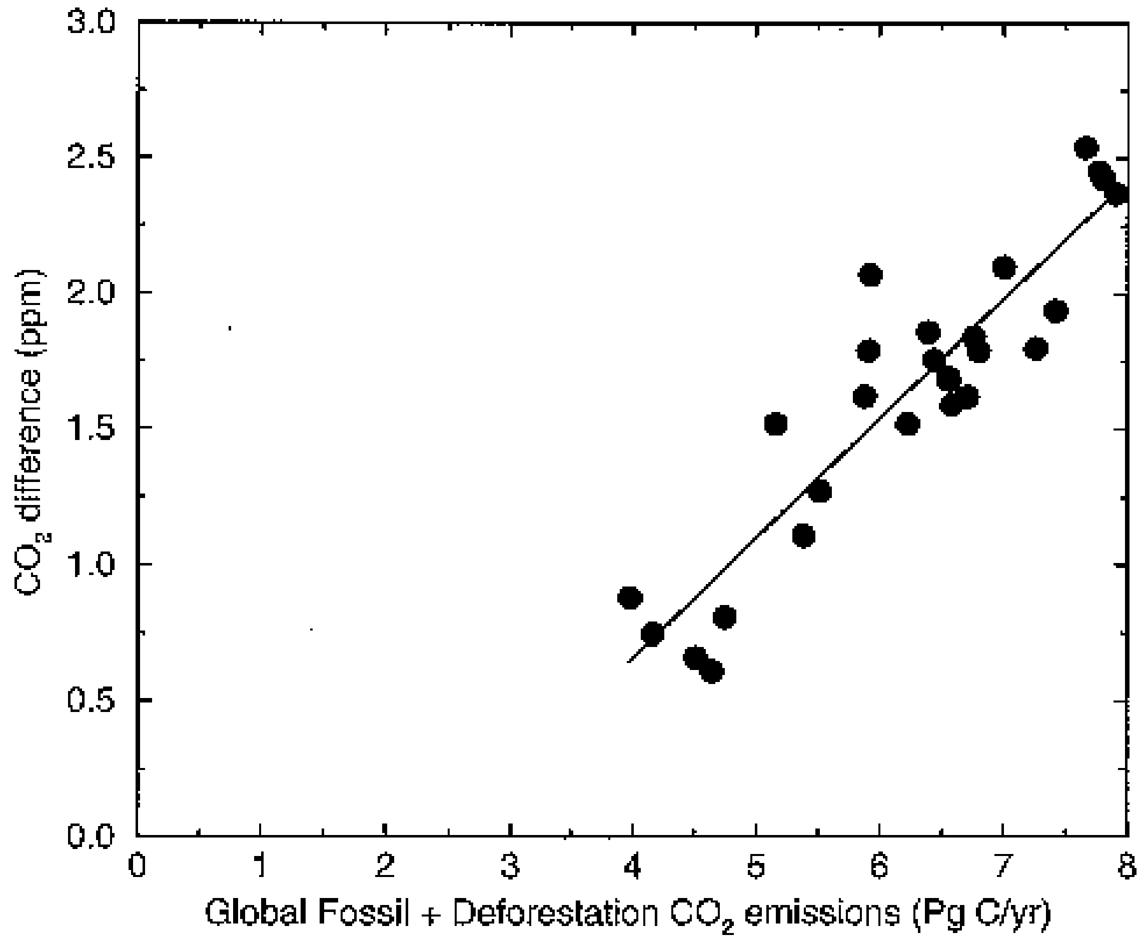
3.0
2.5
2.0
1.5
1.0
0.5
0.0
0
1
2
3
4
5
6
7
8
CO_2 difference (ppm)
Global Fossil + Deforestation CO_2 emissions (Pg C/yr)

Figure 2b

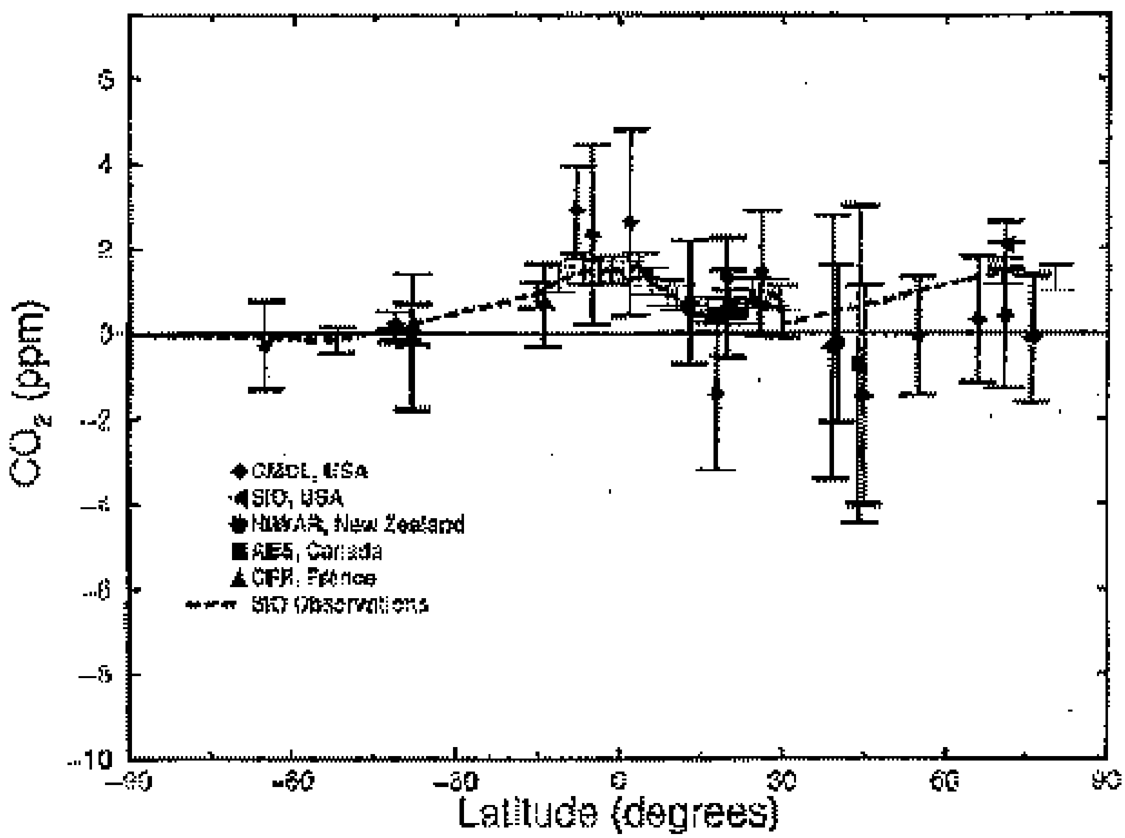
CMDL, USA
SIO, USA
NIWAR, New Zealand
AES, Canada
CFR, France
SIO Observations
CO2 (ppm)
Latitude (degrees)

Figure 3

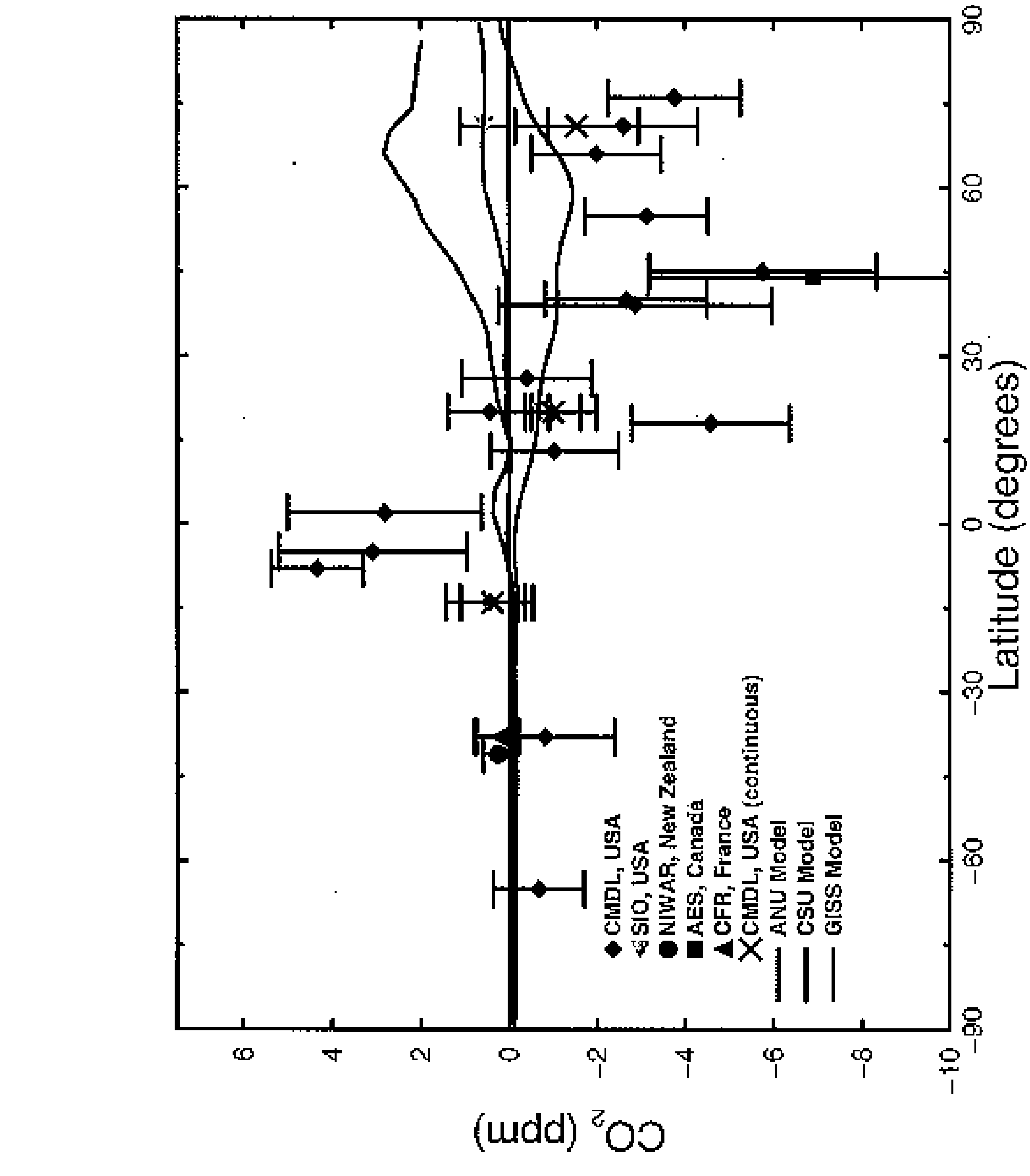
CMDL, USA
SIO, USA
NIWAR, New Zealand
AES, Canada
CFR, France
CMDL, USA (continuous)
ANU Model
CSU Model
GISS Model
Latitude (degrees)
CO_2 (ppm)
−90
−60
−30
0
30
60
90
6
4
2
0
−2
−4
−6
−8
−10

Figure 4a

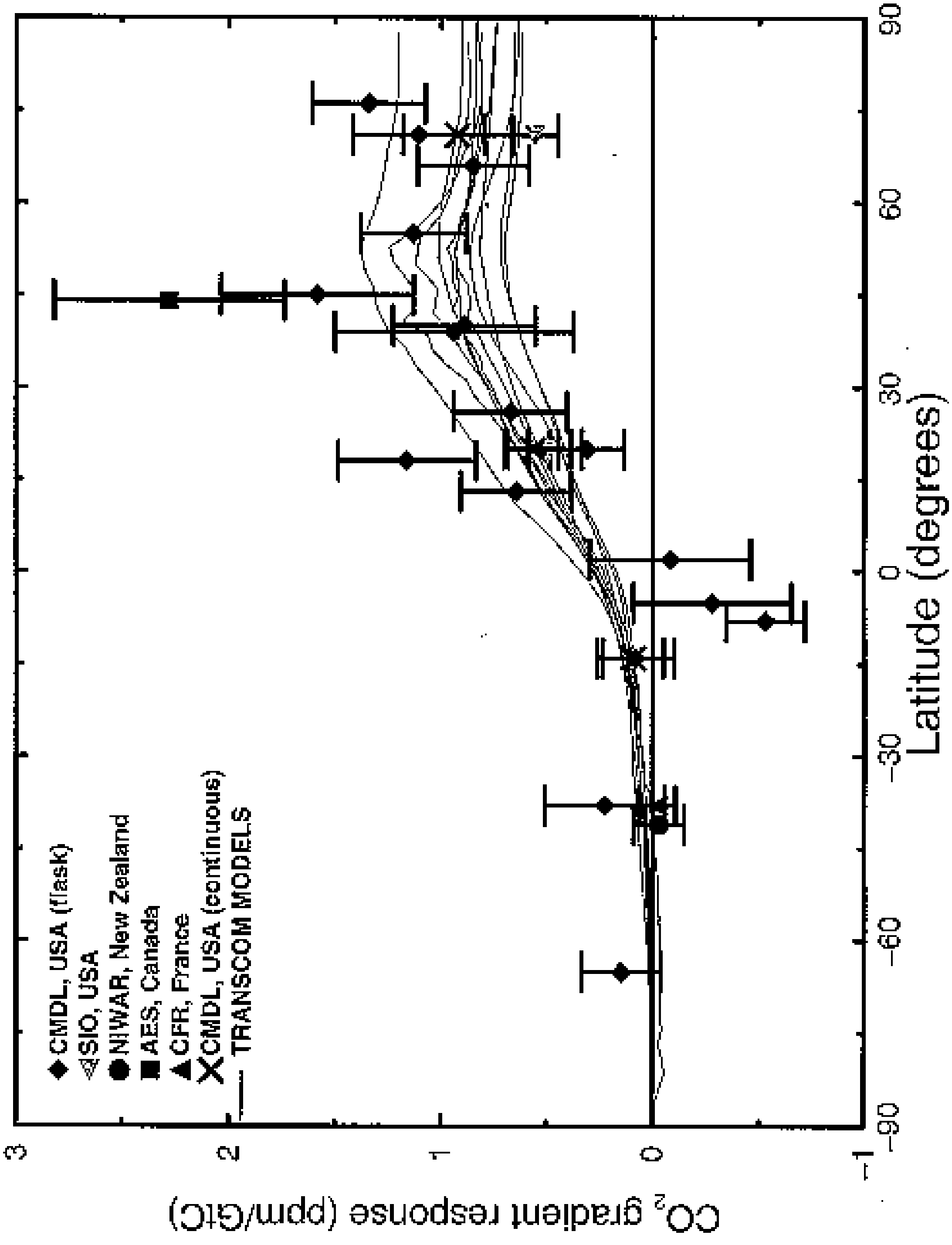
CMDL, USA (flask)
SIO, USA
NIWAR, New Zealand
AES, Canada
CFR, France
CMDL, USA (continuous)
TRANSCOM MODELS
CO_2 gradient response (ppm/GtC)
Latitude (degrees)
−90
−60
−30
0
30
60
90
−1
0
1
2
3

Figure 4b